Int. J. Electrochem. Sci., 15 **(2020)** 8979 – 8989, doi: 10.20964/2020.09.23

International Journal of
ELECTROCHEMICAL
SCIENCE
www.electrochemsci.org

Mechanism of Chromium Electrodeposition from Cr(III) Baths on Nickel and Chromium Electrode Surfaces

Huan Zhao[1,2,], Weihua Liu[2], Qingpeng Li[2], Bo Zhang[2], Jianguo Liu[2], Chuanwei Yan[2], Chunming Liu[1]*

[1] School of Materials Science and Engineering, Northeastern University, Shenyang 110819, China;
[2] Institute of Metal Research, Chinese Academy of Sciences, Shenyang 110016, China
[*]E-mail: hzhao@imr.ac.cn

Received: 16 December 2019 / *Accepted:* 1 June 2020 / *Published:* 10 August 2020

The electrode state changes with the thickening of the coating in Cr(Ⅲ) thick chromium plating. The deposition of Cr(Ⅲ) is carried out on the substrate at the beginning of deposition and on the chromium coating when the chromium coating becomes thicker. The aim of this work is to study the influence of the change of electrode state on the reduction mechanism of trivalent chromium. The electrodeposition mechanism of Cr(III) is studied by cyclic voltammetry, electrochemical impendance spectroscopy, chronoamperometry and polarization technique. The results show that the reduction of Cr(Ⅲ) on chromium coating electrode has a negative deposition potential, higher charge transfer resistance, higher activation energy, and lower diffusion coefficient than those on the nickel electrode, the reduction of Cr(Ⅲ) is more difficult on chromium coating electrode. The change of electrode state is one of the reasons for the difficulty in thickening of chromium coating.

Keywords: Trivalent chromium; Hard chromium electrodeposition mechanism; Nickel electrode; Chromium coating electrode;

1. INTRODUCTION

The chromium coating has been widely used for "decorative chromium" and "hard chromium" in modern equipment due to its beautiful appearance, high hardness, exclusive wear and corrosion resistance[1-3]. The traditional chromium coating electrodeposited from hexavalent chromium baths which are harmful to human and environment[4-6], has been restricted by many countries and regions[7-10]. The replacement of hexavalent chromium from all processes is an imperative.

Trivalent chromium plating is one of the best options to replace hexavalent chromium and has been used to replace hexavalent decorative chromium for many years[11-14]. However, the thick coating is difficult to obtain in trivalent chromium baths which limits its application in hard chromium. The reasons for the difficulty are generally believed that the intense hydrogen evolution reaction

occurs with the reduction of Cr(III), which leads to the rapid increase of OH^- near the cathode. This OH^- increase is responsible for the formation of Cr(Ⅲ) hydroxyl-bridge polymer. The trivalent chromium ion cannot be reduced when the hydroxyl bridge compounds are formed[15-19].

The thickness of coating is usually more than 30 μm in "hard chromium deposits". During hard chromium deposits progress, not only the concentration of hydroxide ion near the cathode changes, but also the surface of the electrode changes. The deposition of Cr(III) is carried out on the substrate at the beginning of the deposition and on the chromium coating when the chromium coating becomes thicker. The change of electrode will affect the deposition mechanism of Cr(III). The deposition mechanism of trivalent chromium has been extensively studied on glassy carbon electrode, steel electrode, copper electrode and gold electrode[20-25], has not yet been studied on chromium coating electrode. The deposition of chromium coating is usually carried out on the surface of nickel substrate in the actual electroplating process, so nickel electrode and chromium coating electrode are used as working electrode in this work.

The objective of this work is to study the nucleation process and electrodeposition mechanism at different stages of thick chromium deposition from trivalent chromium plating bath. The electrochemical behavior on nickel electrode and chromium coating electrode are studied by means of cyclic voltammetry, electrochemical impendance spectroscopy, constant potential step and polarization.

2. MATERIAL AND METHODS

2.1 Preparation of chromium coating electrode

Trivalent chromium coating was deposited from solution which compared of 0.8 mol/L chromium chloride, 0.2 mol/L formic acid, 0.3 mol/L boric acid, 1.0 mol/L sodium chloride, 2.0 mol/L urea, 0.08 mol/L sulfuric acid and 200 ml/L methyl alcohol. The solution was made up with deionized water (18.2 MΩ·cm) and analytical grade purity reagent. The pH of solution was adjusted to 1.0~1.2 with sodium hydroxide or hydrochloric acid. A nickel rod (φ15×70 mm) was used as cathode and graphite plate was used as anode. The solution was maintained at 40±2 ℃ during the deposition.

2.2 Electrochemical measurements

All electrochemical experiments were performed with Gamry Instruments Reference 600™ potentiostat/galvanostat and using a three electrode based electrochemical cell. The nickel electrode and chromium coating electrode were used as the working electrode respectively and the large area platinum was used as the counter electrode. The reference electrode was saturated calomel electrode(SCE). The working electrodes were polished with 2000 grit abrasive paper and then in an ultrasonic bath for 5min in order to clean the surface of electrodes. All electrochemical experiments were carried out at 25±2 ℃ if there was no special instruction.

Cyclic voltammetry (CV) was scanned from – 0.22 V to – 1.4 V on 0.015 cm^2 nickel electrode and from – 0.3 V to – 1.6 V on 0.04 cm^2 chromium coating electrode, the scanning rate was

200mV/s. Electrochemical impedance spectra (EIS) was performed at the potential of – 0.7 V in the frequency range from 100 kHz to 0.1 Hz. The amplitude of the sinusoidal voltage signal was 5 mV (peak to peak). The area of working electrodes was 0.5 cm^2 in EIS test.

The surface morphology was observed by Philips XL-30FEG microscope scanning electron microscope (SEM).

3. RESULTS AND DISCUSSION

3.1 Cyclic voltammetry

Cyclic voltammograms are obtained on nickel electrode (Figure 1a) and chromium coating electrode (Figure 1b) with the scan rate of 200 mV/s. Cyclic voltammetry are measured in plating solution with and without Cr(III) respectively to confirm the reduction peak of Cr(III). No reduction peak is found above – 1.3 V in the solution without Cr(III). However, an obvious reaction peak appears at – 0.92 V in the solution with Cr(III) on nickel electrode, which can be considered as the reduction peak of Cr(III). The curves on the chromium coating electrode are similar to that on the nickel electrode, but the reduction peak appears at – 1.26 V and the peak current is much smaller. Compared to the nickel electrode, the potential of reaction peak on the chromium electrode is negative and the peak of current is low, indicate that Cr(III) is difficult to reduce on chromium coating electrode than on nickel electrode. The cyclic voltammetry curves of two electrodes don't show obvious oxidation peak during the retrace process, which indicate that the reduction of Cr(III) is irreversible.

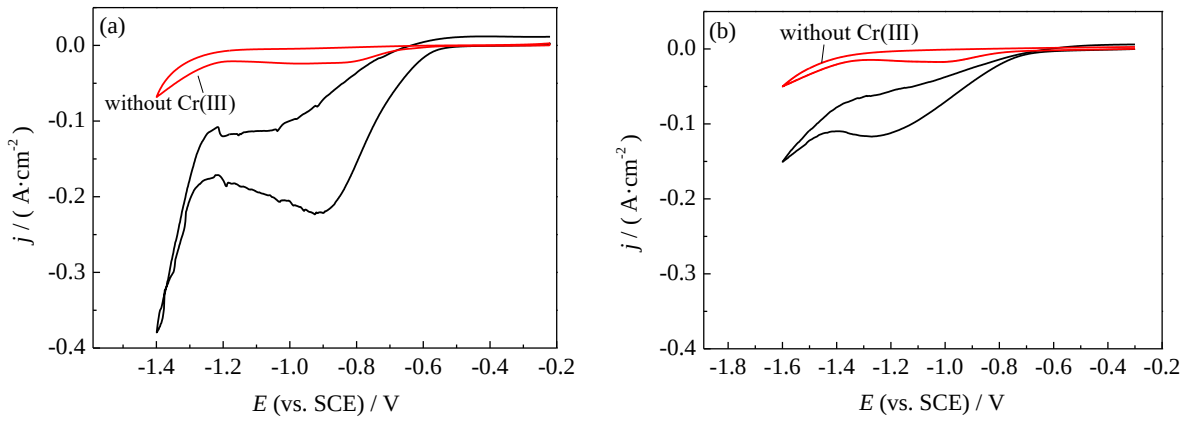

Figure 1. Cyclic voltammograms obtained on (a) Nickel electrode; (b) Chromium coating electrode. (Scan rate 200 mV/s)

3.2 Polarization curve

As shown in Figure 2, the cathodic polarization curve of Cr(III) on nickel electrode can be divided into four stages. The current density remains unchanged before – 0.55 V and there is no electrochemical reaction in this stage. The second stage is between – 0.55 V and – 0.95 V, the current density increase with the negative shift of the potential and indicating that the reduction reaction is

proceed. There is a current platform between – 0.95 V and – 1.3 V, which is known as the reduce reaction of Cr(III) according to the standard electrode potential. The current increases rapidly when the potential is below – 1.3 V, a violent hydrogen evolution reaction has occurred.

The cathodic polarization curve of chromium coating electrode can be divided into two stages. The first stage is above – 0.65 V and the current remains unchanged at this stage. The current increases linearly when the potential is below – 0.65 V, no obvious reaction platform can be observed. It shows that the reduction reaction of Cr(III) on chromium coating electrode is always dominated by electrochemical reaction, and the electrochemical reaction rate is low relatively.

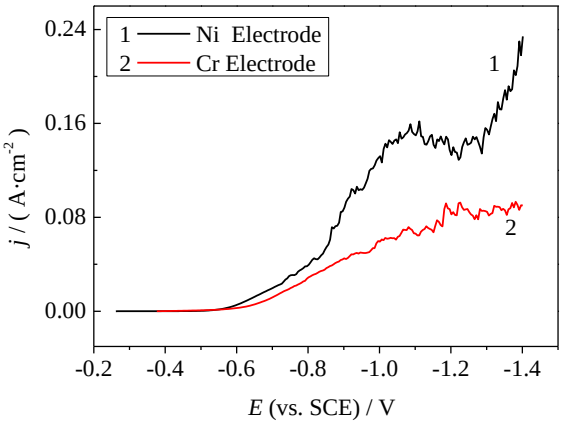

Figure 2. Cathodic polarization curves on nickel and chromium coating electrodes. (Scan rate 2 mV/s)

3.3 Electrochemical impendance spectroscopy (EIS)

Electrochemical impedance spectroscopy is an important method to study electrode kinetics and interface reaction that can provide in-depth information about resistance, double layer capacitance, electrode reaction steps and charge-transport phenomena of a system[26].

EIS experiments are carried out on chromium coatings electrode with the thickness of 0 μm, 10 μm, 30 μm and 50 μm. The electrode with the thickness of 0 μm is nickel electrode. There are two capacitive loops in Nyquist curves of chromium coating electrode with different thickness (Figure 3).

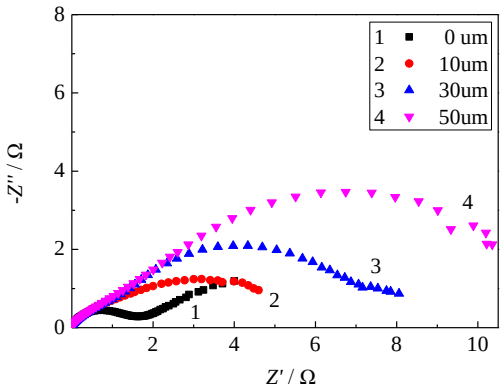

Figure 3. Nyquist on chromium coating electrodes with different thickness at potential of – 0.7 V.

The charge transfer resistance on chromium coating electrode is larger than it on nickel electrode and becomes much larger with the thickness increase of the chromium coating. It exhibits that the reduction reaction of Cr(III) is difficult to carry out on the thick chromium coating, the deposition rate will decrease when the chromium coating grows thicker.

3.4 Activation energy

The reaction rate changes less with the temperature when the electrode reaction is under diffusion-controlled, so the activation energy of the electrode reaction is low, usually from 12 to 16 kJ/mol. The reaction rate changes greatly with the temperature when the electrode reaction is under electrochemical-controlled, and the activation energy of the electrode reaction is usually higher than 40 kJ/mol[27]. Therefore, the control steps of the electrode reaction can be judged by measuring the activation energy of the electrode reaction. The relations between activation energy and temperature can be described as the following equation:

$$\ln j_\eta = B - \frac{E}{RT}$$

where j_η is current density; E is activation energy; T is temperature; R is gas constant; B is a constant when the electrode reaction is constant. From the formula, we can see that there is a linear relationship between $\ln j_\eta$ and $1/T$. The electrode reaction activation energy could be calculated as the described in Reference[28].

Galvanostatic current/voltage characteristics (j-E curves) are obtained by potentiodynamic scan which is performed at different temperatures with the scan rate of 2 mV/s, the results are shown in Figure 4a (nickel electrode) and Figure 4b (chromium coating electrode).

The linear relations between $\ln j_\eta$ and $1/T$ are plotted at reduction potential according to the results of cyclic voltammetry, the peak potential of Cr(III) reduction reaction is －0.92 V on the nickel electrode and －1.26 V on the chromium coating electrode (Figure 5). The calculation results of activation energy are shown in Table 1.

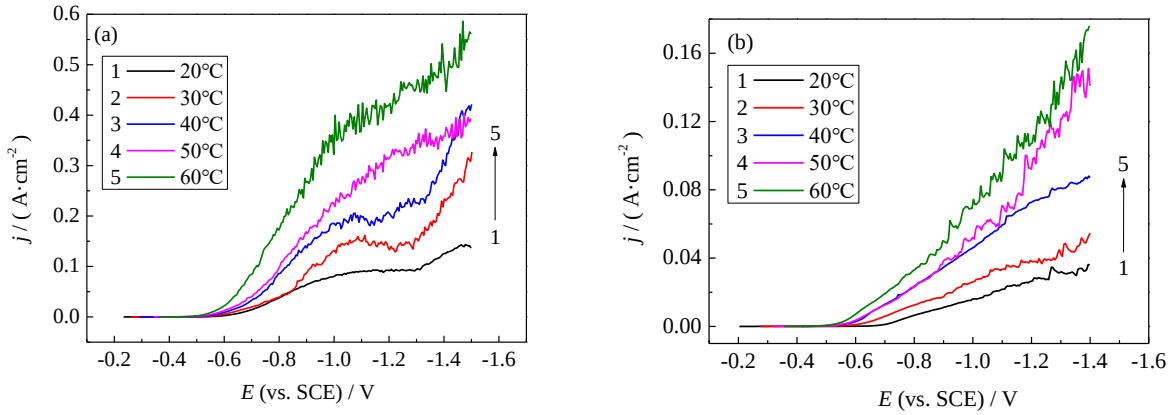

Figure 4. Polarization curves obtained on (a)Nickel electrode; (b)Chromium coating electrode. (Scan rate 2 mV/s)

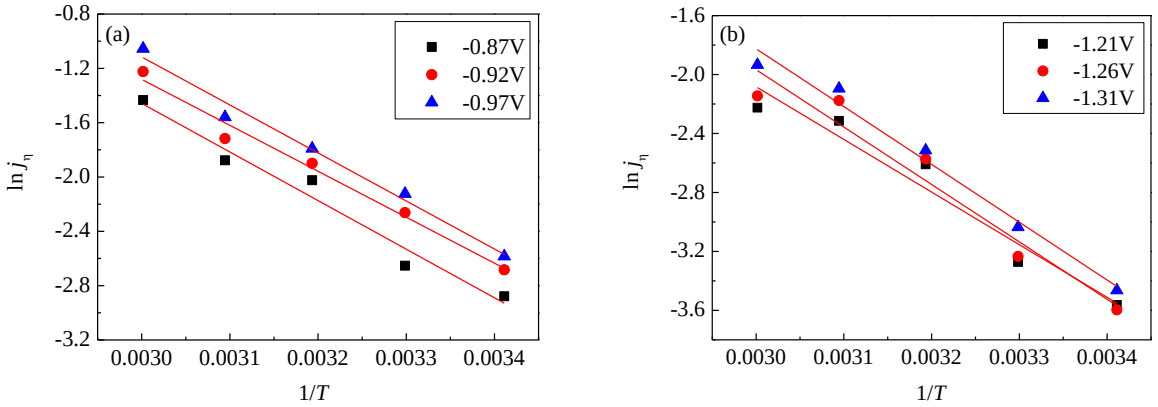

Figure 5. Correlation between lnj_η and 1/T on (a) Nickel electrode; (b) Chromium coating electrode.

Table 1. Electrode reaction activation energy of Cr(III) on nickel and chromium coating electrodes

	Potential /V	Activation energy /kJ·mol^{-1}	Average Value /kJ·mol^{-1}
Nickel electrode	- 0.87	29.75	29.19
	- 0.92	28.44	
	- 0.97	29.40	
Chromium coating electrode	- 1.21	29.69	31.56
	- 1.26	32.38	
	- 1.31	32.61	

The activation energy of Cr(III) on chromium coating electrode is bigger than it on the nickel electrode, indicating that the reaction of Cr(III) is more difficult to occur on the chromium coating. The activation energy of both nickel and chromium coating electrodes are larger than 16 kJ/mol and less than 40 kJ/mol, so the reduction process of Cr(III) is controlled by diffusion and electrochemical reaction together.

3.4 Chronoamperometry

The electrodeposition of metal involves two processes, one is that the metal ions gain electrons from the electrodes and undergo a reduction reaction, the other is the electrocrystallization process in which the newly formed metal atoms form a new phase on electrode surface. The formation and growth mode of crystal nuclei during electrocrystallization have a great influence on the density, brightness and mechanical strength of the coating. Therefore, it is significative to study the electrocrystallization behavior during metal electrodeposition.

Chronoamperometry is an important electrochemical technique used to probe the nucleation and growth mechanism. A number of models have been developed to describe the *J*–*t* curves[29-30]. There is no doubt that the model developed by Scharifker[31] is accepted widely. The *J*–*t* curves can be described as the following equation:

Instantaneous: $I = \frac{nFD^{\frac{1}{2}}C}{(\pi t)^{\frac{1}{2}}}[1-\exp(-N\pi KDt)]$

$$K = \left(\frac{8\pi CM}{\rho}\right)^{\frac{1}{2}}$$

Progressive: $I = \frac{nFD^{1/2}C}{(\pi t)^{1/2}}[1-\exp\left(-\frac{AN\pi K'Dt^2}{2}\right)]$

$$K' = \frac{4}{3}\left(\frac{8\pi CM}{\rho}\right)^{1/2}$$

Where, I is the current, t is time, N is the number of nuclei, D is the diffusion coefficient, C is the concentration, F is Faraday constant, A is the nucleation rate constant, M is the molar mass of the depositing species, ρ is the density of depositing species.

There are instantaneous nucleation and progressive nucleation according to the model. Instantaneous nucleation occurs at a small number of active sites with a slow growth of nuclei, all active sites activated at the beginning of the deposition. Progressive nucleation corresponds to a fast growth of nuclei on many active sites and the active sites activated during the course of reduction[32].

Chronoamperometry experiments are performed at the reduction potentials of Cr(Ⅲ), －0.8 V, －0.9 V, －1.0 V and －1.1 V on nickel electrode, －1.1 V, －1.2 V, －1.3 V and －1.4 V on the chromium coating electrode. The potential step time is 60 s. It is found that the current changes only at the moment when the potential is stepped, and then remains constant. For a clearer reflection of the current variation, only the data of initial 5 s are collected . The time-current curves obtained on nickel and chromium coating are shown in Figure 6.

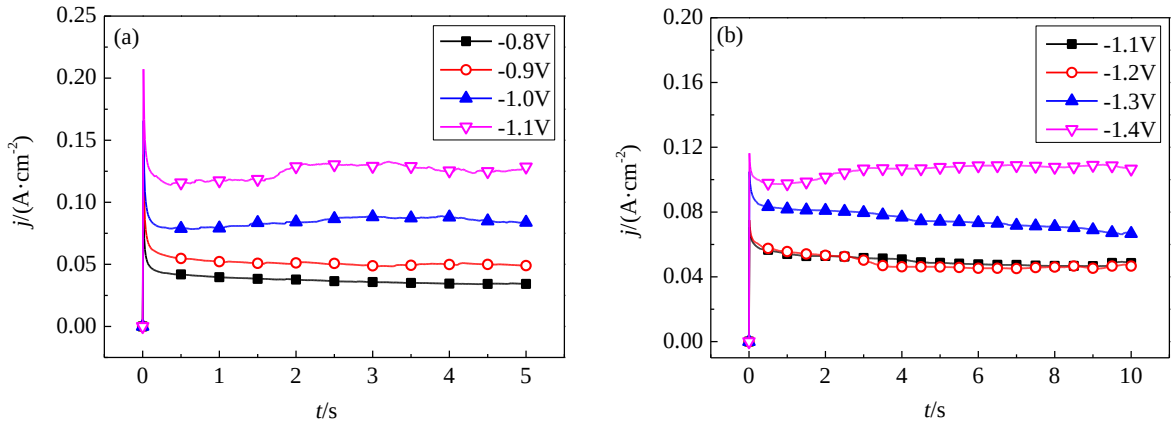

Figure 6. Time-current curves on (a) Nickel electrode; (b) Chromium coating electrode.

There is a maximum current in the *J-t* curves which indicates a typical nucleation process [33]. The maximum currents appear at the moment of potential stepped and then decrease to a steady value in a short time. The steady current on chromium coating electrode is lower than it on the nickel electrode at the same potential, the reduction of Cr(Ⅲ) on chromium coating electrode is more difficult than it on nickel electrode.

The corresponding fit of experimental data according to Scharifker's model is presented in

Figure 7. The theoretical curves of three-dimensional instantaneous nucleation and progressive nucleation are also plotted as reference.

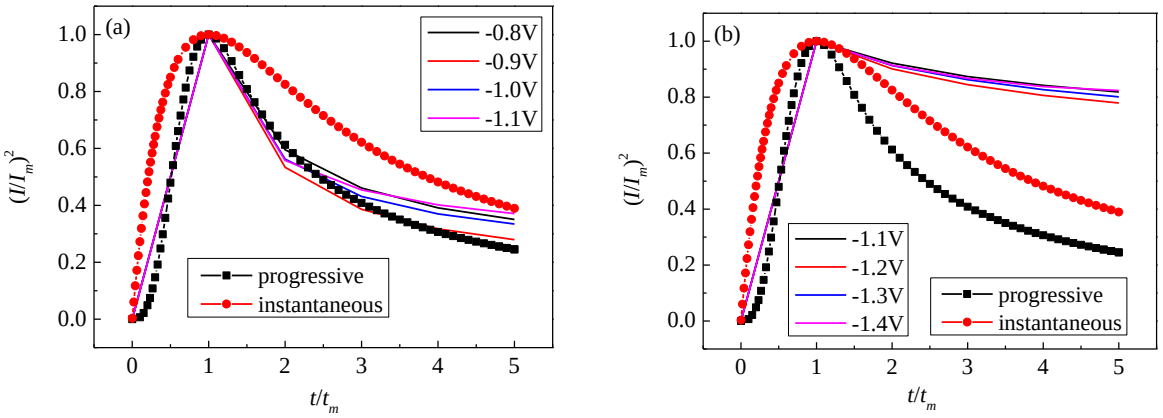

Figure 7. Nondimensional plots of $(I/I_m)^2$ — t/t_m curves corresponding Scharifker's (a) Nickel electrode; (b) Chromium coating electrode.

The nucleation mechanism of Cr(III) on nickel electrode follows the progressive nucleation model at the beginning of the deposition, and shifts toward the instantaneous nucleation mode with time. The departure from progressive nucleation mechanism is at about $t/t_m = 2.5$. The nucleation mechanism of Cr(III) on chromium coating electrode does not fit the nucleation model of Scharifker. The deviation between the experimental curves and the theoretical curves is attributed to the fact that the model of Scharifker is developed based on the hypothesis of diffusion-controlled[34], but the reaction rate of Cr(III) is mainly under electrochemical-controlled, and the electrode reaction rate is slow.

The diffusion coefficient of chromium and number of crystal nucleus can be calculated according to the model of Scharifker[35]. The results are shown in Table 2.

Table 2. Diffusion coefficient and crystal nucleus number density of Cr(III) on nickel and chromium coating electrode

	E / V	I_m / 10^{-2} A·cm^{-2}	t_m / s	D / 10^{-8} cm^2·s^{-1}	N /10^9 cm^{-2}
Nickel electrode	- 0.8	9.14	0.01	0.96	11.00
	- 0.9	13.85	0.01	2.20	4.79
	- 1.0	16.60	0.01	3.15	3.33
	- 1.1	20.72	0.01	4.91	2.14
Chromium coating electrode	- 1.1	5.82	0.01	0.39	27.09
	- 1.2	7.50	0.01	0.65	16.32
	- 1.3	10.49	0.01	1.26	8.35
	- 1.4	11.63	0.01	1.55	6.80

On the same electrode, the peak current and the diffusion coefficient increase with the negative shift of the step potential, but the nucleation number density decreases gradually. It is well known that the negative shift of step potential will increase the driving force of the electrochemical reaction, so the diffusion coefficient of Cr(III) increase. High overpotential will lead to the increase of concentration polarization which can limit the formation of the nucleus. Moreover, high overpotential will cause the reaction of hydrogen evolution, the generation and escape of hydrogen bubbles on the surface of the electrode is not favorable for the stability of the nucleus[36]. Therefore, the nucleation number density decreases gradually at high overpotential.

At the same step potential, the nucleation density of Cr(III) on chromium coating electrode is larger than that on nickel electrode. This may be caused by the micropores and microcracks on the surface of the chromium coating, which are beneficial to the formation of crystal nucleus. Another reason for the difference in the electrocrystallization mechanism may be the crystal matching of the crystal nucleus and the substrate crystal structure[37], nickel belongs to the face centered cubic crystal structure, and chromium belongs to the body centered cubic crystal structure, Cr(Ⅲ) is easier to nucleate on the chromium coating electrode and the nucleation number density is larger.

Cr(III) is electrodeposited on nickel electrode at the beginning of the hard chromium electroplating, when follows the progressive nucleation theory and the diffusion coefficient of Cr(III) is much larger. When the electrode surface is covered with chromium coating completely, the electrocrystallization of Cr(III) changes from progressive nucleation to instantaneous nucleation, and the diffusion rate decreases, resulting in a slow increase in coating thickness.

No chromium nuclei is observed on nickel electrode (Figure 8a), but the chromium has been deposited on nickel electrode from EDS analysis (Figure 8b). The chromium nuclei can be observed clearly on chromium coating electrode (Figure 8c).

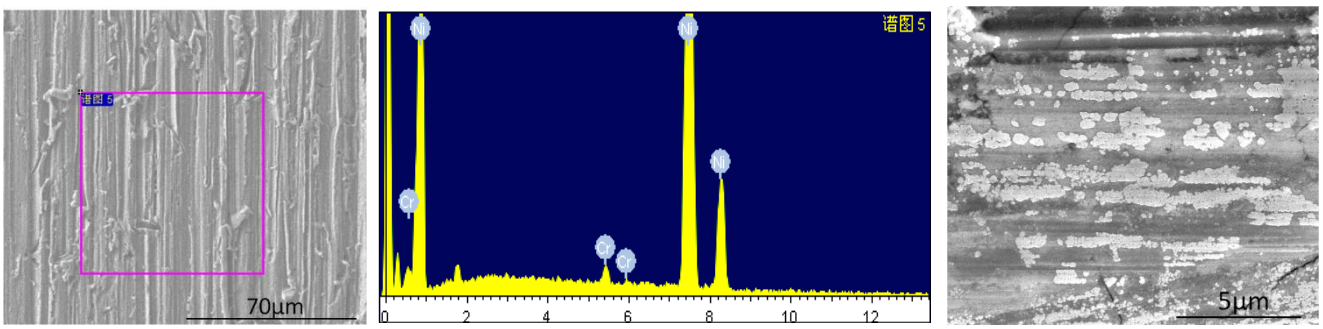

(a) (b) (c)

Figure 8. (a) SEM image of deposit formed on nickel electrode; (b) EDS analysis of deposit coating on nickel electrode; (c) SEM image of deposit formed on chromium coating electrode.

4. CONCLUSION

The nucleation mechanism and reduction mechanism of Cr(III) on the nickel electrode and chromium coating electrode are studied in this paper. The nucleation mechanism of Cr(Ⅲ) on nickel electrode follows the progressive nucleation model at the beginning of the deposition, and shifts

toward instantaneous mode with deposition time. The nucleation mechanism on chromium coating electrode does not fit the nucleation model of Scharifker. At the same stepped potential, the diffusion coefficient on chromium coating electrode is smaller than that on nickel electrode but the nucleation density is higher. Compared with nickel electrode, the reduction of Cr(III) on chromium coating electrode has a negative deposition potential, higher charge transfer resistance, higher activation energy, and lower diffusion coefficient, indicate the reduction of Cr(III) is more difficult to carried out on chromium coating electrode.

The change of electrode state is one of the reasons for the difficulty in thickening of chromium coating. This suggests that the consistent current regime throughout the whole electroplating process is inappropriate for hard chromium electroplating. A suitable current regime should be established for the reduction characteristics of Cr(III) at different electroplating stages.

References

1. V. S. Protsenko and F. I. Danilov, *Clean Techn. Environ. Policy,* 16 (2014) 1201.
2. O. V. Safonova, L. N. Vykhodtseva, N. A. Polyakov and J. C. Swarbrick, *Electrochim. Acta*, 56 (2010) 145.
3. H. F. Alesary, A. F. Khudhair, S. Y. Rfaish and H. K. Ismail, *Int. J. Electrochem. Sci.,* 14 (2019) 7116.
4. J.H. Lindsay, *Plat. Surf. Finish.,* 8 (2004) 16.
5. Y.B. Song and D.T. Chin, *Electrochim. Acta,* 48 (2002) 349.
6. C.A. Huang, Y.W. Liu, C. Yu and C.C. Yang, *Surf. Coat. Technol.,* 205 (2011) 3461.
7. W. Zhang and C.W. Wu, *Mater. Prot.,* 46 (2013) 38.
8. C.W. Guo and J. Lai, *Total Corrosion Control,* 25 (2011) 46.
9. D. D. Pianta, C. Gleyzes, C. Cugnet, J.C. Dupin and I.L. Hecho. *Electrochim. Acta,* 284 (2018) 234.
10. Q. Cheng and Y.D. He, *Surf. Coat. Technol.,* 269 (2015) 319.
11. J.P. Hoare, *Electrochem. Soc.* 126 (1979) 190.
12. A. Baral and R. Engelken, *J. Electrochem. Soc.,* 152 (2005) 504.
13. V. S. Protsenko and F. I. Danilov, *Electrochim. Acta,* 54 (2009) 5666.
14. A.M. Liang, L. W. Ni, Q. Liu and J. Y. Zhang, *Surf. Coat. Technol.,* 218 (2013) 23.
15. Z. M. Tu and Z. L. Yang, *Plat. Surf. Finish.,* 79 (1993) 78.
16. V.N. Korshunov, V.A. Safonov and L.N. Vykhodtseva, *Russ. J. Electrochem.,* 44 (2008) 255.
17. S.K. Ibrahim, D.T. Gawne and A. Watson, *Trans. IMF.,* 76 (1998) 156.
18. N.V. Mandich, *Plat. Surf. Finish.,* 84 (1997) 97.
19. N.V. Mandich, *Plat. Surf. Finish.,* 84 (1997) 108.
20. E. S.C. Ferreira, C.M. Pereira and A.F. Silva, *J. Electroanal. Chem.,* 707 (2013) 52.
21. V.S. Protsenko, F.I. Danilov, V.O. Gordiienko, S.C. Kwon, M. Kim and J.Y. Lee, *Thin Solid Films,* 520 (2011) 380.
22. X. K. He, B. L. Hou, C. Li, Q.Y. Zhu, Y. M. Jiang and L. Y. Wu, *Electrochim. Acta,* 130 (2014) 245.
23. R. Giovanardi and G. Orlando, *Surf. Coat. Technol.,* 205 (2011) 3947.
24. V. S. Protsenko, V. O. Gordiienko and F. I. Danilov, *Electrochem. Commun.,* 17 (2012) 85.
25. N. V. Phuong, S. C. Kwon, J. Y. Lee, J. Y. Shin, B. T. Huy and Y. I. Lee, *Microchem. J.*, 99 (2011) 7.
26. A.M. Alberto, M.S. Teresa, G.D. Liliance and F.M. Maria, *Electrochim. Acta,* 289 (2018) 47.

27. X.G. Shu, L.W. Liao, X. Z. He and H.M. Huang, *Surface Technology,* 39 (2010) 13.
28. M. Suermann, T. J. Schmidt, and F. N. Büchi, *Electrochim. Acta,* 281 (2018) 466.
29. R. D. Armstrong and J. A. Harrison, *J. Electrochem. Soc.* 116 (1969) 328.
30. E. Budevski, W. Bostanoff, T. Witanoff , Z. Stoiroff, Z. Kotzewa, R. Kaischew, *Electrochim. Acta,* 11 (1966) 1697.
31. B. Scharifker and G.Hills, *Electrochim. Acta,* 28 (1983) 879.
32. M.P. Pardave, M.T. Ramirez, I. Gonzales, A. Serruya and B.R. Scharifker, *J. Electrochem. Soc.,* 143 (1996) 1551.
33. F.Z. Yang, G.M. Cao, X. Hu, S.K. Xu and S.M. Zhou, *Electrochemistry,* 5 (2000) 169.
34. M. Gu, F.Z. Yang, L. Huang, S. B. Yao and S.M. Zhou, *Acta Chim. Sinica,* 60 (2000) 1946.
35. A. Basile, A. I. Bhatt, A. P. O'Mullane, S. K. Bhargava, *Electrochim. Acta,* 56 (2011) 2895.
36. D. Grujicic and B. Pesic, *Electrochim. Acta,* 47 (2002) 2901.
37. M. Gu and X. H. Xian, *Prog. in Chem.,* 20 (2008) 483.